Electronic Supplementary Material (ESI) for Catalysis Science & Technology.
This journal is © The Royal Society of Chemistry 2017

Electronic Supplementary Information

Effect of Introducing Fe_2O_3 into CeO_2-ZrO_2 on Oxygen Release Property and Catalytic Methane Combustion over PdO/CeO_2-ZrO_2-Fe_2O_3/γ-Al_2O_3 Catalysts

Minchan JEONG, Naoyoshi NUNOTANI, Naoki MORIYAMA, and Nobuhito IMANAKA*

Department of Applied Chemistry, Faculty of Engineering, Osaka University,

2-1 Yamadaoka, Suita, Osaka, 565-0871, Japan

**imanaka@chem.eng.osaka-u.ac.jp*

Experimental

Catalyst preparation

$Ce_{0.68}Zr_{0.17}Fe_{0.15}O_{2-\delta}/\gamma\text{-}Al_2O_3$ (CZF/Al_2O_3) samples were synthesized using the conventional wet coprecipitation method. Before preparation, commercial $\gamma\text{-}Al_2O_3$ (AxSorbAB, Nippon Light Metal Company, Ltd.) powder was ground in an agate mortar and then mechanically pulverized by a ball-milling apparatus (Pulverisette 7, FRITSCH GmbH) at a rotation speed of 300 rpm for 3 h. Aqueous solutions of 1.0 $mol\cdot L^{-1}$ $Ce(NO_3)_3$, 0.1 $mol\cdot L^{-1}$ $ZrO(NO_3)_2$, and 0.1 $mol\cdot L^{-1}$ $Fe(NO_3)_3$ were mixed with 15 mL of 3 $mol\cdot L^{-1}$ nitric acid in stoichiometric amounts. The solution was then impregnated on the $\gamma\text{-}Al_2O_3$ powder. The mixture was stirred at room temperature for 30 min. The pH of the aqueous mixture was adjusted to 11 by dropwise addition of 6% ammonia. After stirring for 12 h at room temperature, the resulting precipitate was collected by filtration, washed several times with deionized water, and then dried at 80 °C for 6 h. Subsequently, these powders were calcined at 500 °C for 1 h under ambient air atmosphere. Samples of palladium supported on CZF/Al_2O_3 were prepared by the impregnation of $Pd(NO_2)_2(NH_3)_2$ solution (Tanaka Kikinzoku Kogyo K.K.) into the CZF/Al_2O_3 samples. Subsequently, the catalysts were dried at 80 °C for 12 h and then calcined at 400 °C for 4 h. The amounts of PdO and CZF were adjusted in the range of 8.0–13.6 wt% and 0–25 wt%, respectively. In addition, 11.3 wt% PdO/16 wt% $Ce_{0.8(1-x)}Zr_{0.2(1-x)}Fe_xO_{2-\delta}/\gamma\text{-}Al_2O_3$ (x = 0, 0.1, 0.2) catalysts were synthesized by the same method. For comparison, 11.3 wt% PdO /16 wt% $Ce_{0.68}Zr_{0.17}Bi_{0.15}O_{2-\delta}/\ \gamma\text{-}Al_2O_3$ catalyst was also prepared by the same coprecipitation and impregnation methods using 0.5 $mol\cdot L^{-1}$ $Bi(NO_3)_3$ instead of 0.1 $mol\cdot L^{-1}$ $Fe(NO_3)_3$. In addition, 11.3 wt% PdO/$Ce_{0.68}Zr_{0.17}Fe_{0.15}O_{2-\delta}$ (PdO/CZF) and 11.3 wt% PdO/$Ce_{0.8}Zr_{0.2}O_{2-\delta}$ (PdO/CZ) solids were prepared by the coprecipitation and impregnation methods identical with the above methods without using $\gamma\text{-}Al_2O_3$ support. For the Rietveld analysis, $Ce_{0.68}Zr_{0.17}Fe_{0.15}O_{2-\delta}$ (CZF), $Ce_{0.68}Zr_{0.17}Bi_{0.15}O_{2-\delta}$ (CZB), and $Ce_{0.8}Zr_{0.2}O_{2-\delta}$ (CZ) solids were prepared by the coprecipitation method identical with the above method without using $\gamma\text{-}Al_2O_3$ support, and the powders were calcined at 700 °C for 1 h.

Characterization

X-ray photoelectron spectroscopy (XPS; PHI5000 VersaProbe II, ULVAC-PHI) was performed at room temperature using Al Kα radiation. The effect of charging on the binding energies was corrected with respect to the C 1s peak at 284.6 eV, and spectra were fitted using a Shirley background and a Gaussian–Lorentzian line shape. X-ray fluorescence (XRF; ZSX100e, Rigaku Corp.) was used to determine the compositions of the catalysts. X-ray powder diffraction (XRD; SmartLab, Rigaku Corp.) patterns were measured with Cu Kα radiation (40 kV, 30 mA) in the 2θ range from 10° to 70° with a step size of 0.02° and a scan speed of $2^{\circ}\cdot\mathrm{min}^{-1}$. For Rietveld analysis, XRD data (MultiFlex, Rigaku Corp.) were also recorded in the 2θ range from 10 to 150° with a step size of 0.02° for a count time of 5 sec using Cu Kα radiation (40 kV, 40 mA). Structural parameters, such as the lattice parameter and oxygen occupancy, were determined by Rietveld refinements with RIETAN-FP software.[23] Brunauer–Emmett–Teller (BET) specific surface area was measured by nitrogen adsorption at −196 °C (TriStar 3000, Shimadzu Corp.). Temperature-programmed reduction (TPR) measurement was carried out under a flow of 5 vol% hydrogen–argon ($50\ \mathrm{mL}\cdot\mathrm{min}^{-1}$) at a heating rate of $5\ ^{\circ}\mathrm{C}\cdot\mathrm{min}^{-1}$ up to 500 °C (BELCAT-B, MicroTracBEL). The oxygen storage capacity (OSC) was measured using the pulse-injection method at 427 °C. Before the injection of oxygen, the catalyst was out gassed under a helium flow. Pluses of oxygen ($50\ \mathrm{mL}\cdot\mathrm{min}^{-1}$) were injected into the helium ($50\ \mathrm{mL}\cdot\mathrm{min}^{-1}$) passing through the catalyst until the breakthrough point was attained, and the total OSC value was estimated as the uptake of oxygen from the oxygen pulse by comparing the thermal conductivity detection (BELCAT-B, MicroTracBEL).

The methane oxidation activity was tested in a conventional fixed-bed flow reactor consisting of a quartz glass tube (diameter = 10 mm) with a feed gas mixture of 1 vol% methane–air at a rate of $33.4\ \mathrm{mL}\cdot\mathrm{min}^{-1}$ over 0.1 g of catalyst. Here, the space velocity was $20{,}000\ \mathrm{L}\cdot\mathrm{kg}^{-1}\cdot\mathrm{h}^{-1}$. The catalysts were pretreated at 200 °C for 2 h under argon flow ($20\ \mathrm{mL}\cdot\mathrm{min}^{-1}$) prior to the catalytic activity tests. The catalytic activity was evaluated in terms of methane conversion. The gas composition after the reaction was analyzed using gas chromatography with thermal conductivity detection (GC-8AIT, Shimadzu Corp.).

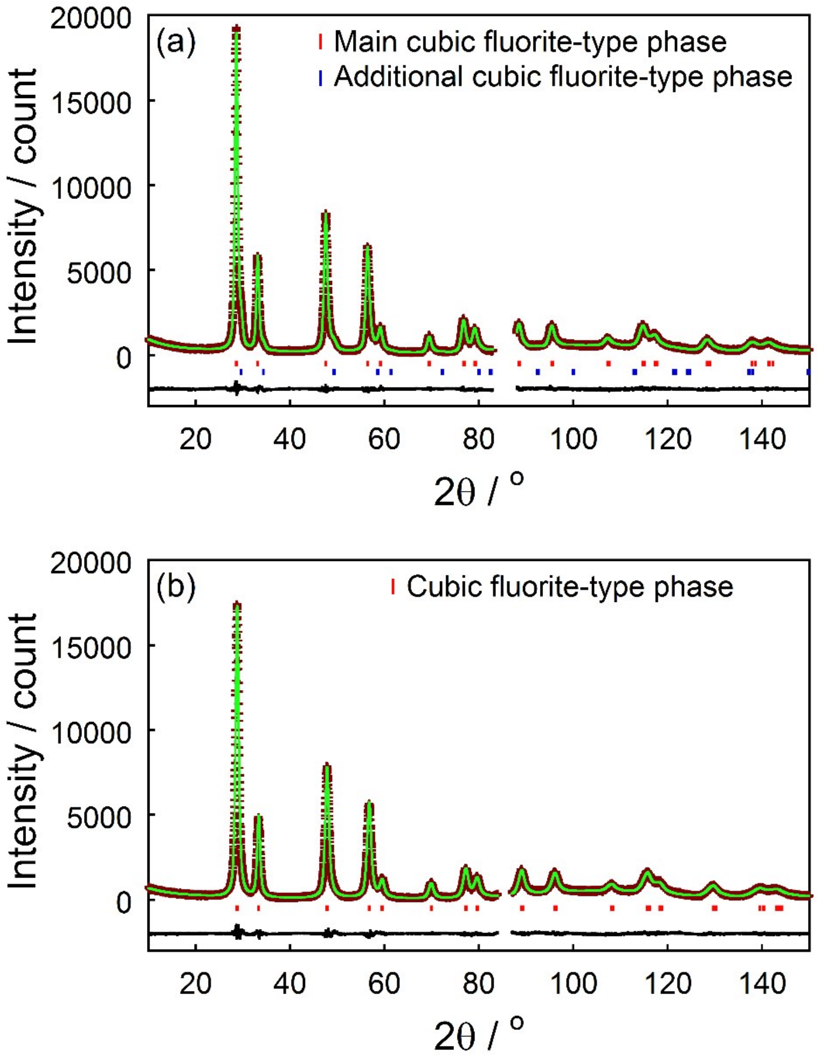

Figure S1. Results of Rietveld analyses of (a) CZB and (b) CZ.

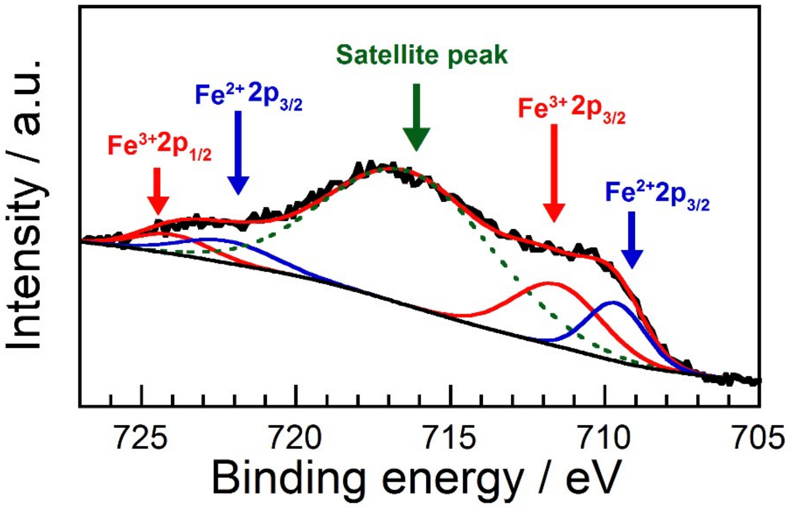

Figure S2. XPS spectrum of Fe 2p core-levels of CZF. Fe 2p$_{3/2}$ and Fe 2p$_{1/2}$ peaks can be assigned to divalent Fe^{2+} (709.6 and 722.2 eV) and trivalent Fe^{3+} (711.6 and 724.0 eV) and the peak at 716.4 eV is identified as a satellite peak.[28-30]

.

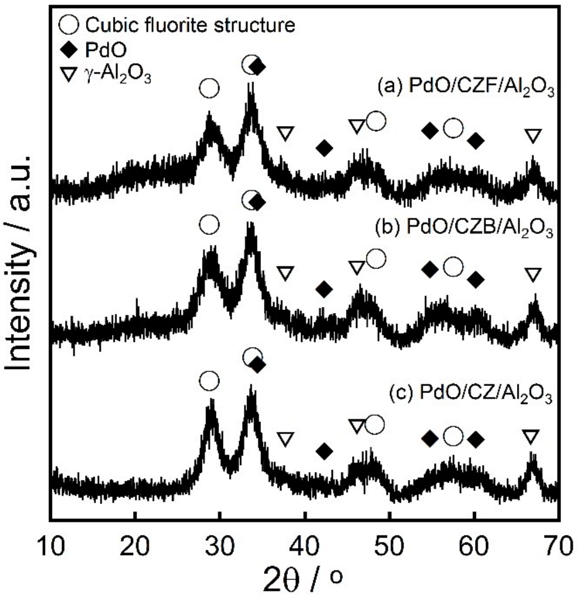

Figure S3. XRD patterns of (a) PdO/CZF/Al_2O_3, (b) PdO/CZB/Al_2O_3, and (c) PdO/CZ/Al_2O_3.

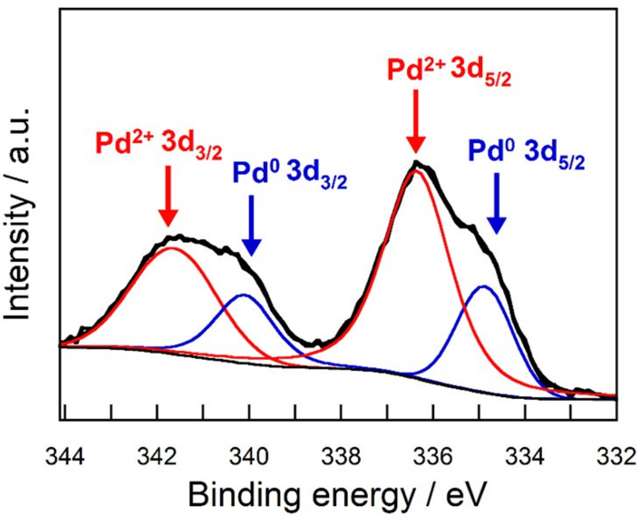

Figure S4. XPS spectrum of Pd 3d core-levels of PdO/CZF/Al_2O_3. The binding energies of Pd $3d_{5/2}$ and $Pd_{3/2}$ can be assigned to divalent Pd^{2+} (336.3 and 341.6 eV) and metallic Pd^0 (334.9 and 340.1 eV).[34,35] The Pd^{2+}:Pd^0 ratio was calculated to be 71:29.

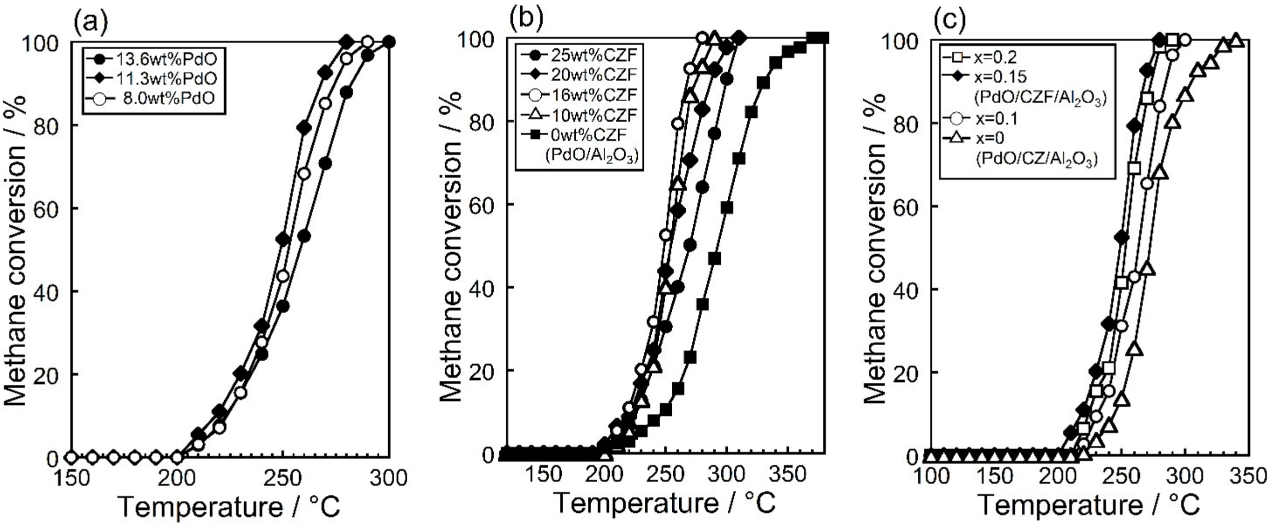

Figure S5. Temperature dependencies of methane conversion of (a) (8.0–13.6) wt% PdO/16 wt% CZF/Al_2O_3, (b) 11.3 wt% PdO/(0–25) wt% CZF/Al_2O_3, and (c) 11.3 wt% PdO/16 wt% $Ce_{0.8(1-x)}Zr_{0.2(1-x)}Fe_xO_{2-\delta}/\gamma\text{-}Al_2O_3$ ($0 \leq x \leq 0.2$).

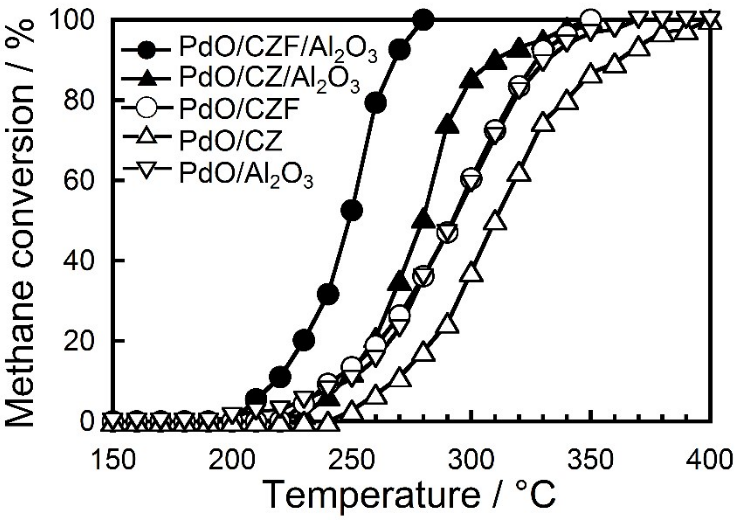

Figure S6. Temperature dependencies of methane conversion of PdO/CZF/Al_2O_3, PdO/CZ/Al_2O_3, PdO/CZF, PdO/CZ, and PdO/Al_2O_3.

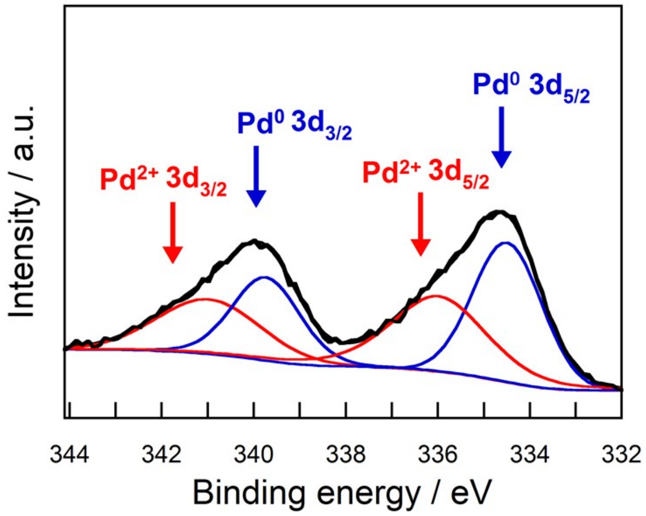

Figure S7. XPS spectrum of Pd 3d core-levels of PdO/CZ/Al_2O_3. The binding energies of Pd 3d$_{5/2}$ and Pd$_{3/2}$ can be assigned to divalent Pd^{2+} (336.0 and 341.0 eV) and metallic Pd^0 (334.5 and 339.7 eV).[34,35] The Pd^{2+}:Pd^0 ratio was calculated to be 39:61.